Mammalian mad2 and bub1/bubR1 recognize distinct spindle-attachment and kinetochore-tension checkpoints

Dimitrios A. Skoufias*†, Paul R. Andreassen*†, Françoise B. Lacroix*, Leslie Wilson‡, and Robert L. Margolis*§

*Institut de Biologie Structurale J.-P. Ebel (Commissariat à l'Energie Atomique–Centre National de la Recherche Scientifique), 41 Rue Jules Horowitz, 38027 Grenoble Cedex 1, France; and ‡Department of Molecular, Cellular, and Developmental Biology, University of California, Santa Barbara, CA 93120

Communicated by J. Richard McIntosh, University of Colorado, Boulder, CO, February 15, 2001 (received for review September 17, 2000)

Metaphase checkpoint controls sense abnormalities of chromosome alignment during mitosis and prevent progression to anaphase until proper alignment has been attained. A number of proteins, including mad2, bub1, and bubR1, have been implicated in the metaphase checkpoint control in mammalian cells. Metaphase checkpoints have been shown, in various systems, to read loss of either spindle tension or microtubule attachment at the kinetochore. Characteristically, HeLa cells arrest in metaphase in response to low levels of microtubule inhibitors that leave an intact spindle and a metaphase plate. Here we show that the arrest induced by nanomolar vinblastine correlates with loss of tension at the kinetochore, and that in response the checkpoint proteins bub1 and bubR1 are recruited to the kinetochore but mad2 is not. mad2 remains competent to respond and is recruited at higher drug doses that disrupt spindle association with the kinetochores. Further, although mad2 forms a complex with cdc20, it does not associate with bub1 or bubR1. We conclude that mammalian bub1/bubR1 and mad2 operate as elements of distinct pathways sensing tension and attachment, respectively.

The proper segregation of chromosomes in anaphase is essential to maintain the integrity of the genome. Metaphase checkpoint controls at the kinetochore can sense failure of spindle attachment or of spindle tension and thereby assure accurate chromosome segregation. The proteins mad1, mad2, mad3, bub1, bub3, and mps1 are linked to the spindle checkpoint in budding yeast (1, 2). Genetic analysis in yeast suggests a hierarchy among the different checkpoint control proteins, with bub1 and mps1 upstream of mad1 and mad2, which in turn are upstream of mad3; however, data do not rule out the existence of multiple pathways (3). Homologues of yeast checkpoint proteins, such as mad2 (4, 5), bub1 (6), and bubR1 (7), are present in vertebrates. mad2, bub1, and bubR1 are all required for checkpoint control in higher eukaryotes (4–8). mad2 appears to sense microtubule attachment to kinetochores in mammalian cells (9). It is unknown, however, whether the different elements of metaphase checkpoint control are parts of a single cascade of response or represent independent and parallel sensing mechanisms after distinct failures.

There are known associations among the mammalian kinetochore-associated checkpoint proteins. mad1, a dimer with a coiled-coil motif, binds to mad2 at the kinetochore, forming an association essential to mad2 function (10). mad2 binds to cdc20, one of the proteins required for activation of the anaphase-promoting complex (APC), and indirectly associates with other APC elements through cdc20 (11). Additionally, bub1 and bubR1 appear to require bub3 for kinetochore binding (12). bubR1 appears to be associated in turn with the kinetochore-associated motor protein CENP-E (13, 14) and with APC elements cdc16, cdc27, and APC7 (7).

In addition to the known requirement for mad2 in sensing microtubule attachment at the kinetochore, there is evidence from different nonmammalian sources that tension of microtubules at the kinetochores can also generate a checkpoint response (15–17). HeLa, human cervical cancer cells, arrest at metaphase for prolonged periods of time when exposed to low concentrations of microtubule inhibitors that do not sever the kinetochore–microtubule association (18). Here we demonstrate that the metaphase arrest arising in HeLa in response to nanomolar levels of vinblastine correlates with a loss of spindle tension. Because of their apparent checkpoint response to loss of tension, HeLa cells are ideal for determining the molecular requirements particular to a loss of tension checkpoint response. We find that, in this circumstance, bub1 and bubR1 return to the kinetochores, whereas mad2 does not. Correlating with this distinction in response, we also find that bub1 and bubR1 do not coimmunoprecipitate with mad2, and that mad2 but not bub1 clearly associates with cdc20 in cell extracts. We conclude that mammalian mad2 and bub1/bubR1 operate as elements of distinct pathways in HeLa, sensing attachment and tension, respectively.

Materials and Methods

Cell Culture. HeLa cells were grown as monolayers in DMEM (GIBCO/BRL) supplemented with 10% FBS (HyClone) and maintained in a humid incubator at 37°C in a 5% CO_2 environment.

Cells were grown for a minimum of 48 h to ensure good adherence to the substrate before any treatment. Vinblastine, a generous gift from Eli Lilly Research Laboratories, was kept as a frozen stock in H_20. Nocodazole (Sigma) was dissolved in DMSO and kept frozen until used.

Immunofluorescence Microscopy. HeLa cells were grown on polyD-lysine-coated glass coverslips for immunofluorescence microscopy. Cells were fixed with 1% paraformaldehyde-PBS for 20 min, washed 5 min with PBS, permeabilized with 0.2% Triton X-100 in PBS for 3 min, and washed again for 5 min with PBS, then processed with primary and secondary antibodies and counterstained with propidium iodide, where utilized, as described (19). Rabbit mad2 antiserum, purchased from Babco (Richmond, CA), was diluted 100-fold. Rabbit anti-bub1 and anti-bubR1 antisera, a kind gift from T. Yen (Fox Chase Cancer Institute, Philadelphia), were used at dilutions of 1,000- and 2,000-fold, respectively. Results for bub1 were confirmed with an independent antibody (data not shown) obtained from F. McKeon (Harvard Medical School, Boston) and used at a 200-fold dilution after fixation with absolute methanol for 10 min at −20°C. Secondary antibodies, from Jackson ImmunoResearch, included FITC-conjugated affinity purified goat anti-

Abbreviations: APC, anaphase promoting complex; VBL, vinblastine; L-VBL, low (6.7 nM) VBL; GFP, green fluorescent protein.

†D.A.S. and P.R.A. contributed equally to this work.

§To whom reprint requests should be addressed. E-mail: margolis@ibs.fr.

The publication costs of this article were defrayed in part by page charge payment. This article must therefore be hereby marked "*advertisement*" in accordance with 18 U.S.C. §1734 solely to indicate this fact.

www.pnas.org/cgi/doi/10.1073/pnas.081076898

rabbit IgG, anti-mouse IgG, and anti-human IgG; and Texas red-conjugated sheep anti-mouse IgG antibodies. All antibodies were applied at 2.5 μg/ml. Images were collected with a MRC-600 Laser Scanning Confocal Apparatus (Bio-Rad) coupled to a Nikon Optiphot microscope.

Measurement of Distances Between Paired Sister Kinetochores. Cells were grown on glass coverslips. Control metaphases were selected from random cultures. Experimental conditions included treatment with either 6.7 nM vinblastine (VBL) for 20 min to suppress microtubule dynamics or with 0.5 μM VBL for 20 min to depolymerize microtubules. Cells were fixed with 2% paraformaldehyde–PBS for immunofluorescence microscopy, permeabilized as above, then incubated with scleroderma CREST (calcinosis, Raynaud's phenomenon, esophageal dysmotility, sclerodactyly, telangiectasia) autoimmune antiserum (M. Wener, University of Washington) to identify centromeres and with antitubulin antibodies (Sigma) to identify metaphase figures (19). Optical sections were imaged by confocal microscopy, and the distance between paired kinetochores was measured by using COMOS software (Bio-Rad). For each treatment condition, all kinetochore pairs resolvable in an optical section were measured from the outer edge of each kinetochore in a pair, and data were accumulated for 15 cells. Our methodology for measurement of interkinetochore distances with and without tension was similar to that previously reported for taxol treatment (20), and values were comparable to previous measurements in HeLa (21).

Immunoprecipitation and Immunoblotting. To assay whether bub1 and bubR1 associate with mad2, extracts were prepared from mitotic cells selectively detached after incubation with 0.33 μM nocodazole for 4 h. For the preparation of extracts, cells were centrifuged, washed with PBS at 4°C, and lysed in 50 mM Tris·HCl (pH 7.5)/150 mM NaCl/1% Nonidet P-40/10% glycerol/2 mM EDTA containing 50 mM NaF, 0.5 mM β-glycerolphosphate, 0.1 mM PMSF, 10 μg/ml aprotinin, and 10 μg/ml leupeptin. Lysate supernatants were then collected by centrifugation at 13,000 $\times$ *g*. For immunoprecipitation, 2.0 μg of mad2 antiserum was added to 50 μg of extracted protein and incubated for 1 h at 4°C with agitation. Protein G-Sepharose beads were then added for 1 h at 4°C with agitation. The protein–antibody complex was washed three times with lysis buffer. After immunoprecipitation, samples were resolved by 15% PAGE for the detection of mad2 and on 8% gels for the detection of bub1 and bubR1. Electrophoresis, transfer to nitrocellulose, blocking, and washes were as described (19). For the detection of proteins on nitrocellulose, antibodies to mad2, bub1, and bubR1 antibodies were diluted 1,000-, 5,000-, and 2,000-fold, respectively. After exposure to horseradish peroxidase-conjugated goat anti-mouse IgG secondary antibody (Kirkegaard & Perry Laboratories; diluted 5,000-fold) for 1 h, blots were washed and developed by enhanced chemiluminescence (Pierce).

To compare the levels of mad2, bub1, and bubR1 after suppression of microtubule dynamics or microtubule depolymerization, mitotic HeLa cells treated with 6.7 nM VBL, or 0.5 μM VBL, or 1.7 μM nocodazole for 4 h were collected by selective detachment. Interphase cells were grown as subconfluent populations and left untreated. Extracts were prepared as described (19). For each sample, 10 μg of cell extracts was resolved by PAGE, transferred, incubated with primary antibodies, and detected by chemiluminescence as described above. For Western blots of mad2 solubility, cell extracts were prepared as above, except that 0.1% Nonidet P-40 was used, and centrifugation was performed for 5 min at 16,000 $\times$ *g*.

Photon Counting. The confocal microscope was precalibrated to photon counting mode and set by using the highest kinetochore fluorescence signal (high VBL treatment). Twenty scans were made in accumulation mode of different cells under identical machine settings for the mad2 antigen and 10 scans for bub1 and bubR1. Pixel values were obtained for invariant square areas that encompassed kinetochores visualized with the different specific antibodies, and these values were collected as data sets for each of the conditions from at least 10 different cells. For mad2 measurements, a mad2 polyclonal antibody (9), kindly provided by Ted Salmon (University of North Carolina), was used, and these cells were first permeabilized then fixed to reduce background before analysis, by published protocols (9). For mad2, collected at metaphase or in low drug, a diffuse background was present at the position of the chromosomes, with no discrete concentrations of antigen. This background, which was consistent for all conditions, was subtracted from all kinetochore pixel values for mad2 plots.

Microinjection. HeLa cells were grown on polyD-lysine-coated coverslips for at least 3 days before microinjection. Affinity purified and concentrated anti-XMAD2 antibodies at concentrations suitable for microinjection (9) (0.4 mg ml^{-1} in 50 mM K-glutamate, 0.5 mM $MgCl_2$) were kindly provided by Ted Salmon. Antibodies were microinjected into untreated metaphase cells and into metaphase cells treated with low VBL for 30 min by using an inverted phase contrast microscope (Zeiss Axiovert 135 with a heated stage) and an Eppendorf Transjector 5246 microinjection apparatus. Each coverslip was microinjected over a 10-min period. Cells were returned to an incubator for 30, 60, or 120 min, then fixed for 10 min in absolute methanol. Injected cells were identified by immunofluorescence microscopy by using a goat anti-rabbit–FITC-conjugated secondary antibody, and the mitotic state of injected cells was determined by propidium iodide, as described above.

Results

HeLa cells given nanomolar concentrations of VBL arrested indefinitely in mitosis (18). After 20 min of drug exposure, mitotic cells displayed a normal metaphase chromosome array and a bipolar spindle (Fig. 1*A*). Chromosomes remained attached to the spindle, but spindle dynamics were dampened, eliminating microtubule tension at kinetochores. As a result of loss of tension, sister kinetochore distances diminished substantially (44%) from control values (Fig. 1*B*), yielding average values equivalent to those previously reported for kinetochores of spindles in which microtubule dynamics had been entirely suppressed (21) and to values obtained when spindles were destroyed by high VBL (Fig. 1*B*).

From the above, it is apparent that HeLa cells contain a metaphase checkpoint that responds to lack of spindle tension. To seek the molecular correlate of this tension checkpoint, we examined the response of three checkpoint proteins, bub1, bubR1, and mad2, to low concentrations of VBL.

Different drug treatment conditions did not substantially alter the overall abundance of the three checkpoint proteins in mitotic cells (Fig. 1*C*). Differences observed in localization of checkpoint proteins could thus be attributed to their local rather than global concentrations. During a normal metaphase, bub1 and bubR1 were barely detectable, and mad2 was not visibly detectable at kinetochores, as determined by immunofluorescence microscopy (Fig. 2*A*). When spindle tension was eliminated at metaphase by treatment of HeLa cells with 6.7 nM VBL [low VBL (L-VBL)] for 20 min, the signals for bub1 and bubR1, but not mad2, increased at the kinetochores in metaphase arrays (Fig. 2*A*). Off-plate chromosomes were rare in the cell population arrested with L-VBL for 20 min. Images were collected with constant confocal microscope settings, standardized to normal metaphases for each antigen. We obtained identical results with an independently raised bub1 antibody (data not shown).

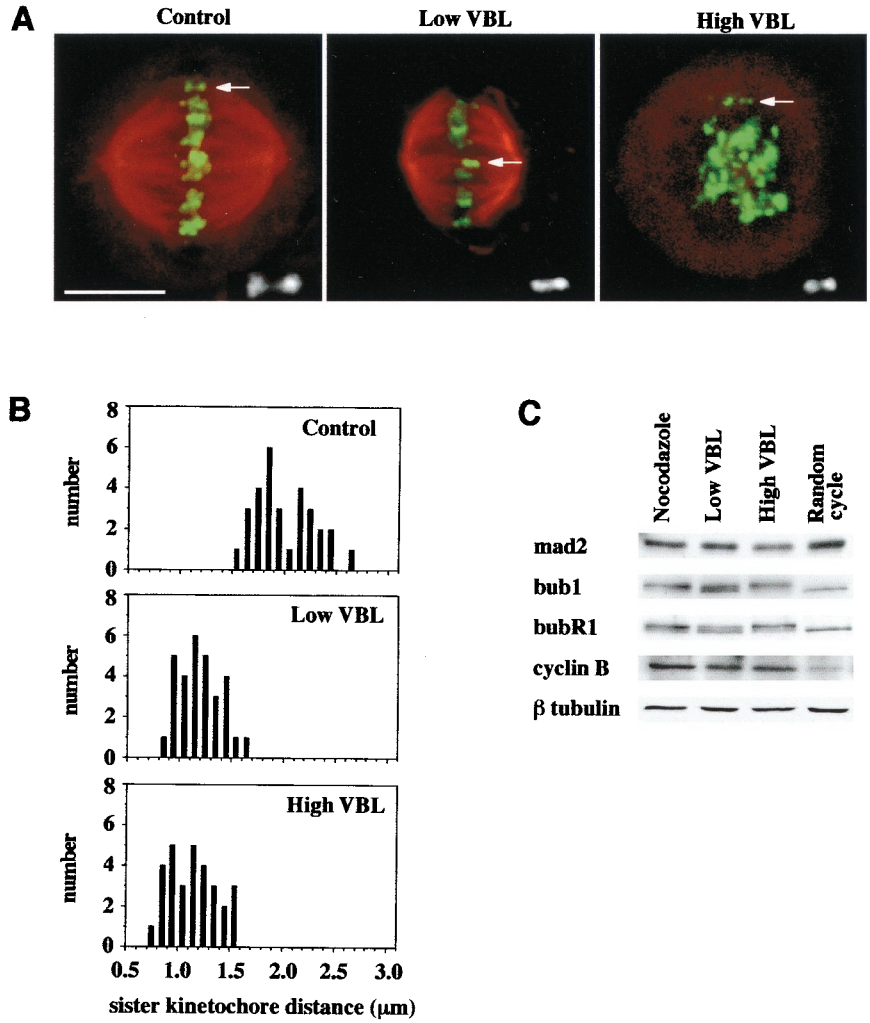

Fig. 1. Treatment of HeLa cells with low concentrations of vinblastine suppresses microtubule dynamics while maintaining a bipolar mitotic spindle and attached kinetochores. (*A*) Double-label immunofluorescence microscopy for centromeres (green; detected with CREST variant scleroderma human autoimmune serum) and antitubulin (red) demonstrates that 6.7 nM VBL does not perturb bipolar spindle association with kinetochores, as compared with untreated control metaphase cells. By contrast, 0.5 μM VBL induces complete disassembly of the mitotic spindle. (Bar = 10 μm.) *Insets* show enlargements of kinetochore pairs representative of those used for measurements. Point-to-point measurements were made by using COMOS software. Kinetochore pairs were selected by their close proximity, presence in the same focal plane, and, when at metaphase, alignment with the long axis of the spindle. Measured distances of the *Inset* kinetochores shown were: control, 2.04 μm; L-VBL, 1.24 μm; H-VBL, 1.16 μm. (*B*) VBL (6.7 nM) suppresses spindle tension at kinetochores, reducing the distance between sister kinetochores relative to that of untreated control metaphases (from 1.95 $\pm$ 0.28 μm to 1.15 $\pm$ 0.2 μm), yielding values comparable to those in 0.5 μM VBL-treated cells with no spindles (1.1 $\pm$ 0.23 μm). (*C*) The whole cell levels of mad2, bub1, and bubR1, as determined by immunoblotting, remain constant in mitotic cells in which spindle dynamics are suppressed (6.7 nM VBL) or in which the spindle is disassembled (0.5 μM VBL or 1.7 μM nocodazole). Cyclin B blots are shown to confirm mitotic status. β-tubulin blots are shown to confirm equal loading of all extracts.

By contrast, when microtubule attachment was abolished by exposure to high concentrations of VBL, bub1, bubR1, and mad2 all returned to kinetochores (Fig. 2*A*). bub1 and bubR1 signals in this condition appeared similar to those with low VBL, indicating sensitivity principally to spindle tension. The presence of mad2 on kinetochores lacking microtubules demonstrates sensitivity to microtubule attachment, in accord with Waters *et al.* (9) and shows that absence of mad2 signal seen with low drug was not because of loss of mad2 competence to reassociate with kinetochores. All kinetochore displays had similar levels of mad2 in high VBL. We have imaged those that retained metaphase alignment after loss of spindle attachment.

Quantitative analysis of antigen fluorescence at kinetochores by using the photon counting mode of the confocal microscope supports our observations. Confocal images of representative cells (Fig. 2*B Left*) and statistical analysis (Fig. 2*B Right*) are presented for each antigen (Fig. 2*B*). In cells treated with L-VBL, bub1 (middle bar graph) and bubR1 (lower bar graph) were elevated $\approx$3- and 2-fold, respectively, over control metaphase values, although values were somewhat lower than levels in prometaphase or high drug-treated cells. These differences perhaps reflect an additional response of bub1 and bubR1 to lesser microtubule occupancy both in high drug and in prometaphase (22). In contrast, mad2 was visibly undetectable at all kinetochores in control metaphase and in L-VBL-treated cells (Fig. 2*B*, mad2 low VBL image), even though the centrosomes were discernible in the latter case. Because a single unattached kinetochore can activate the spindle checkpoint (23), it is important to note that at metaphase in control or L-VBL-treated cells, not a single kinetochore positive for mad2 was observed in those cells where all of the chromosomes were aligned at the spindle equator. It is interesting to note that mad2 signal is absent even though the average L-VBL-treated kinetochore contains 27% fewer microtubules at 24 h than controls (24). The

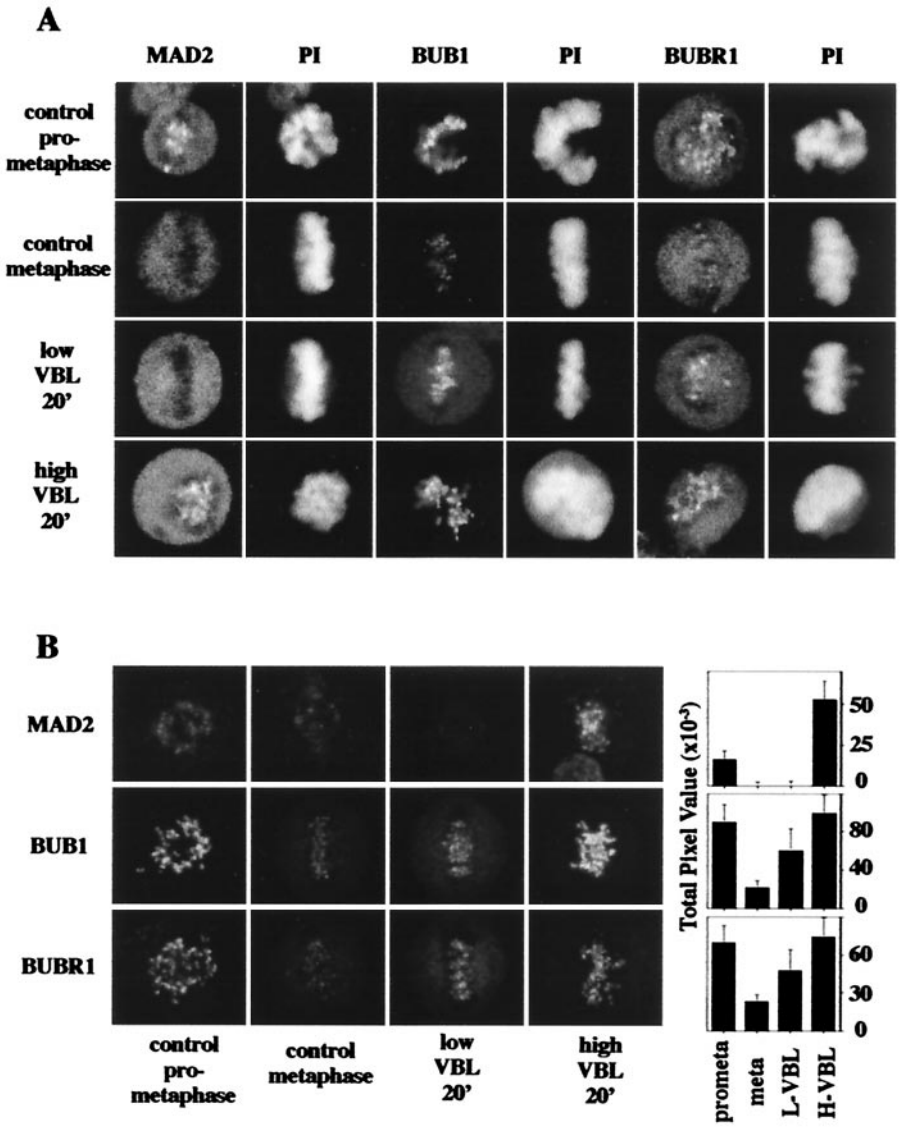

Fig. 2. bub1 and bubR1, but not mad2, respond to the absence of spindle tension by binding to kinetochores. (*A*) mad2 is absent from kinetochores that have attached microtubules and is insensitive to loss of tension by the addition of 6.7 nM VBL for 20 min. In contrast, mad2 reassociates with kinetochores when attachment is abolished by the addition of 0.5 μM VBL. bub1 and bubR1 are minimally detectable at kinetochores of control metaphase cells but reassociate at kinetochores of metaphase arrays when tension is suppressed by the addition of 6.7 nM VBL or if microtubule attachment is abolished by the addition of 0.5 μM VBL. Results were consistent in several independent experiments and (for bub1) with use of two distinct antibodies (data not shown). For each antigen, all images were collected with a confocal microscope by using constant settings established by imaging control metaphases. (Bar = 5 μm.) (*B*) Levels of antigens were quantitated for different conditions by using the photon counting mode of the confocal microscope. (*Left*) The images shown were collected in photon-counting mode at identical machine settings for each antigen. (*Right*) Compiled data for each of the different conditions with at least 300 kinetochores counted for each data set. Standard deviations were as indicated.

bar graph of quantitative pixel counts (Fig. 2*B Right*) corroborates the absence of signal above background. Under identical collection conditions, we obtained reproducible signals in untreated prometaphase cells, where partial microtubule attachment exists, and high signals in cells treated with high drug concentrations, where all microtubule attachments had been destroyed. This insensitivity of mad2 to microtubule saturation at the kinetochore is consistent with the recent argument that a core of microtubules at the late prometaphase kinetochore is sufficient to satisfy the mad2 checkpoint (25).

As bub1/bubR1 and mad2 appear to read different metaphase checkpoints, we expected they would not associate in a complex that could be recruited together to kinetochores. Consistent with this prediction, immunoprecipitates of mad2 from mitotic cells did not exhibit association with either bub1 or bubR1 on crossblots (Fig 3*A*). Essentially all of mad2 was soluble (Fig. 3*B*) and immunoprecipitable (Fig. 3*A*), eliminating the possibility that bub1 or bubR1 were associated with mad2 in a nonextracted fraction. Further, mad2 associated strongly with cdc20 (11, 26), a protein that activates the anaphase promoting complex. Interestingly, although bub1 did not associate with cdc20, bubR1 did appear to be associated (Fig. 3*A*). Failure of bubR1 to associate with mad2 in crossblot analysis is consistent with previous results (14). The checkpoint proteins thus appear to segregate into two distinct groupings.

In further support of our findings, the majority of L-VBL-blocked cells microinjected in metaphase with anti-Xmad2 antibody did not progress to mitotic exit over a 2-h time course (Fig.

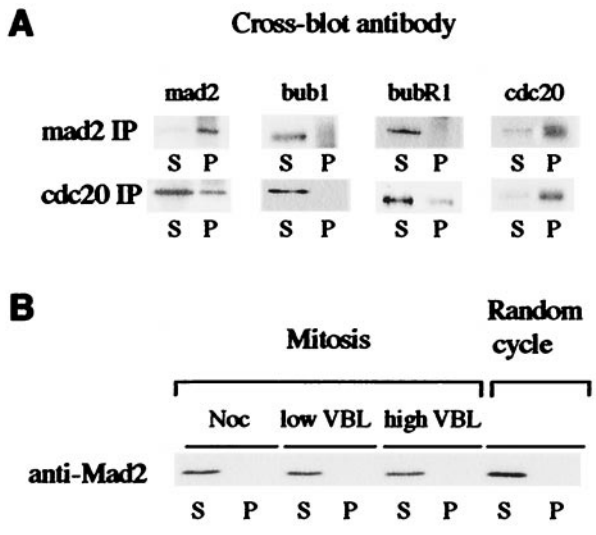

Fig. 3. Associations between mad2, bub1, bubR1, and cdc20. (*A*) Western blots showing neither bub1 nor bubR1 coimmunoprecipitates with mad2 in extracts from mitotic cells (derived by shakeoff after 4-h blockage with nocodazole). Cdc20 coimmunoprecipitates with mad2 and weakly with bubR1 but not with bub1. (*B*) Western blot showing mad2 is entirely soluble in cell extracts. Supernatants (S) and pellets (P) were loaded on the basis of equivalent initial volumes.

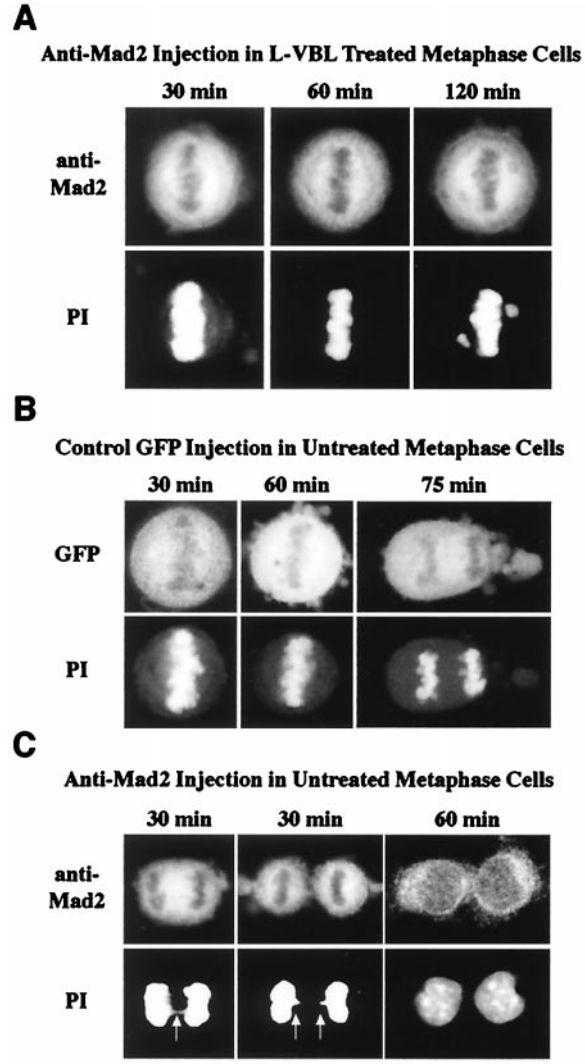

Fig. 4. Response of VLB-treated HeLa to anti-mad2 microinjection. Immunofluorescence micrographs show the result of microinjection of either GFP or anti-mad2 antibody. (*A*) Cells pretreated for 20 min with low VBL (L-VBL) remain in metaphase configuration for at least 2 h (the last time point taken) after microinjection of anti-mad2 antibody. (*B*) GFP microinjection was performed as a positive control in untreated metaphase cells. Shown are representative cells that remain at metaphase for 30 and 60 min, respectively, after microinjection. At later times (an anaphase at 75 min is shown here), cells progress to anaphase and exit mitosis. (*C*) Anti-mad2 microinjection of untreated metaphase cells. In contrast to GFP controls, there is a rapid progression through anaphase and cleavage. Representative cells are shown here 30 min after microinjection in late anaphase and telophase, respectively. The anaphase cells both show evidence of chromosome bridging (arrows), indicating premature entry into anaphase (the propidium iodide stain in both 30-min images has been enhanced to make the bridging visible). GFP or anti-mad2 labels positively identify those cells that had been successfully microinjected. PI, propidium iodide stain to assess the status of the chromosomes after microinjection.

4*A*). Specifically, 17 of 22 VBL-treated injected cells remained in mitosis after 30 min, 13 of 15 were in mitosis after 60 min, and 7 of 11 were in mitosis after 2 h. Although a few cells exited mitosis, the majority of cells did not progress to interphase, as assayed by the lack of the reformed interphase nuclei that were evident in microinjected cells with no drug treatment. The alternative explanation, that the amount of antibody injected is insufficient to override the block, is contrary to our control result, showing that normal metaphase cells display an accelerated exit from mitosis with chromosome bridges, as expected with an active antibody. The criterion we have used for mitotic exit is reformation of interphase nuclei. Note that the times shown in Fig. 4 are maximal estimates for entry into anaphase or telophase or exit from mitosis. Cells could have left metaphase or exited mitosis well before the time points were taken.

Chromatid arm separation, the criterion for mitotic exit used in previous microinjection experiments (9, 27, 28), is unlikely to have occurred in L-VBL-treated injected cells because the majority of cells remained in mitosis after 2 h. The two events, chromatid arm separation and mitotic exit, are linked, as both cyclin B degradation required for mitotic exit and securin degradation required for sister-chromatid separation are mediated by the same cdc20-APC complex (29).

In contrast, all control cells that received no drug treatment and were microinjected with mad2 antibody completed mitosis and entered interphase (as assayed by reformation of interphase nuclei) in less than 60 min, and anaphases and telophases were readily visible at 30 min (Fig. 4 *B* and *C*). The antibody was active in microinjected control cells, as they exited metaphase 30 min earlier than cells injected with a control protein [purified bacterially expressed green fluorescent protein (GFP)], and they commonly contained anaphase bridges (Fig. 4*C*, arrows), as seen in previous microinjection experiments with antibodies directed against kinetochore associated checkpoint proteins (9, 27). With GFP, no anaphase figures appeared until 60 min after injection, and no bridging was evident. The assay for induction of mitotic exit was based on a similar assay by Gorbsky *et al.* (28), and the acceleration of anaphase and telophase was similar to that observed in nondrug-treated PtK1 cells and human keratinocytes after microinjection of mad2 antibodies (27, 28). In addition, the microinjected mad2 antibody strongly recognized kinetochores in mitotic cells whose spindles were destroyed by treatment with 0.33 μM nocodazole (data not shown).

The majority of microinjected L-VBL-treated cells did not exit mitosis in the 2-h time course of this experiment. It is thus clear that a tension-only checkpoint cannot be quickly overcome by mad2 antibody in HeLa. Previous work has shown that checkpoint compromise created by introduction of mad2 antibody (4)

or expression of a dominant negative bub1 mutant (12) led to mitotic exit in HeLa only over a long time course (12–18 h) in high drug concentrations, in contrast to results in PtK1 cells (9). Further work will be required to determine whether the tension-only checkpoint is as durable as the high drug checkpoint in HeLa after compromise of mad2 or bub1 function alone.

Discussion

Our results indicate that, whereas bub1 and bubR1 are responsive to spindle tension, mad2 is not, but, as previously demonstrated (9), mad2 is sensitive to microtubule attachment to the kinetochore. These results suggest that mammalian cells contain at least two discrete checkpoints at metaphase that are independently regulated by different sets of checkpoint proteins. This distinction between checkpoints correlates with the independence of bub1 and bubR1 from mad2 in immunoprecipitates.

We have found that HeLa cells treated with L-VBL do not exit mitosis for at least 2 hours after anti-mad2 microinjection. These results contrast with previous evidence that drug-treated PtK1 cells exit mitosis after microinjection (9, 27, 28). We believe the most reasonable explanation for the discrepancy lies in the difference between cell types chosen for analysis. In contrast to PtK1 cells (30), HeLa cells arrest indefinitely and continue to accumulate in metaphase when exposed to low levels of several different microtubule inhibitors (31). It is because HeLa have a strong tension-dependent checkpoint that they were chosen for the present study.

Our results clarify the nature of the checkpoint mechanism in mammals. It has been unclear whether microtubule attachment or tension, or both, is required for regulation of metaphase arrest. Attachment is an important signal in vertebrate cells, as mad2 binds specifically to unattached kinetochores (9). Tension is required to relieve a metaphase checkpoint in grasshopper spermatocyte meiosis (16). However, a specific requirement for tension has not been previously demonstrated in mammalian cells.

The presence of two distinct assembly and tension checkpoints in vertebrates appears to have an analogue in budding yeast (15), where genetic analysis has demonstrated a clear sensitivity to spindle tension rather than microtubule attachment during meiosis I. In contrast, budding yeast does not appear to activate a kinetochore tension checkpoint in mitosis, as scc1 mutants that lack sister chromatid cohesion go through mitosis with normal kinetics (32). The difference between meiosis I and mitosis may reflect different requirements to avoid nondisjunction in these two cases (15). Our results suggest differences between yeast and mammalian mitotic checkpoint responses. These differences may relate to different spindle mechanisms. In mammals, a poleward flux of microtubules generates tension at the kinetochores (33). No equivalent dynamic appears to operate in yeast. The importance of spindle dynamics and a distinct tension checkpoint in mammals may underlie the specific occurrence of mutations in bub1 and bubR1 in human tumors (8).

Given the respective roles of mad2 and bub1/bubR1 in monitoring spindle attachment and tension, we suggest that mad2 and bub1/bubR1 may be required at different temporal points during a normal mitosis. Both mad2 (34) and bubR1 (7) are required for normal mitotic progression. mad2 may be required before metaphase at a point when not all kinetochores are attached by microtubules to ensure capture of all chromosomes by the spindle; then bub1/bubR1 might act to ensure metaphase alignment of each chromosome after its capture by the spindle.

This paper is dedicated to the memory of Dr. Douglas K. Palmer. We thank Drs. Tim Yen and Frank McKeon for kindly supplying the antibodies used in this work. We are indebted to Dr. Ted Salmon for generously providing purified anti-XMAD2 for microinjection. This work was supported by funding from La Ligue (Laboratoire Labelisé) and Association pour la Recherche sur le Cancer (no. 5338) (R.L.M.) and National Institutes of Health Grant NS13560 (L.W.). L.W. was a Rhône–Alpes fellow, and D.A.S. was supported by a European Molecular Biology Organization fellowship.

1. Li, R. & Murray, A. W. (1991) *Cell* **66,** 519–531.
2. Hoyt, M. A., Totis, L. & Roberts, B. T. (1991) *Cell* **66,** 507–517.
3. Amon, A. (1999) *Curr. Opin. Genet. Dev.* **9,** 69–75.
4. Li, Y. & Benezra, R. (1996) *Science* **274,** 246–248.
5. Chen, R. H., Waters, J. C., Salmon, E. D. & Murray, A. W. (1996) *Science* **274,** 242–246.
6. Taylor, S. S. & McKeon, F. (1997) *Cell* **89,** 727–735.
7. Chan, G. K., Jablonski, S. A., Sudakin, V., Hittle, J. C. & Yen, T. J. (1999) *J. Cell Biol.* **146,** 941–954.
8. Cahill, D. P., Lengauer, C., Yu, J., Riggins, G. J., Willson, J. K., Markowitz, S. D., Kinzler, K. W. & Vogelstein, B. (1998) *Nature (London)* **392,** 300–303.
9. Waters, J. C., Chen, R. H., Murray, A. W. & Salmon, E. D. (1998) *J. Cell Biol.* **141,** 1181–1191.
10. Chen, R. H., Shevchenko, A., Mann, M. & Murray, A. W. (1998) *J. Cell Biol.* **143,** 283–295.
11. Kallio, M., Weinstein, J., Daum, J. R., Burke, D. J. & Gorbsky, G. J. (1998) *J. Cell Biol.* **141,** 1393–1406.
12. Taylor, S. S., Ha, E. & McKeon, F. (1998) *J. Cell Biol.* **142,** 1–11.
13. Chan, G. K., Schaar, B. T. & Yen, T. J. (1998) *J. Cell Biol.* **143,** 49–63.
14. Yao, X., Abrieu, A., Zheng, Y., Sullivan, K. F. & Cleveland, D. W. (2000) *Nat. Cell Biol.* **2,** 484–491.
15. Shonn, M. A., McCarroll, R. & Murray, A. W. (2000) *Science* **289,** 300–303.
16. Li, X. & Nicklas, R. B. (1995) *Nature (London)* **373,** 630–632.
17. Yu, H. G., Muszynski, M. G. & Kelly Dawe, R. (1999) *J. Cell. Biol.* **145,** 425–435.
18. Jordan, M. A., Thrower, D. & Wilson, L. (1991) *Cancer Res.* **51,** 2212–2222.
19. Andreassen, P. R. & Margolis, R. L. (1994) *J. Cell. Biol.* **127,** 789–802.
20. Waters, J. C., Skibbens, R. V. & Salmon E.D. (1996) *J. Cell Sci.* **109,** 2823–2831.
21. Shelby, R. D., Hahn, K. M. & Sullivan, K. F. (1996) *J. Cell Biol.* **135,** 545–557.
22. McEwen, B. F., Heagle, A. B., Cassels, G. O., Buttle, K. F. & Rieder, C. L. (1997) *J. Cell Biol.* **137,** 1567–1580.
23. Rieder, C. L., Cole, R. W., Khodjakov, A. & Sluder, G. (1995) *J. Cell Biol.* **130,** 941–948.
24. Wendell, K. L., Wilson, L. & Jordan, M. A. (1993) *J. Cell Sci.* **104,** 261–274.
25. King, J. M. & Nicklas, R. B. (2000) *J. Cell Sci.* **113,** 3815–3823.
26. Fang, G., Yu, H. & Kirschner, M. W. (1998) *Genes Dev.* **12,** 1871–1883.
27. Canman, J. C., Hoffman, D. B. & Salmon, E. D. (2000) *Curr. Biol.* **10,** 611–614.
28. Gorbsky, G. J., Chen, R.-H. & Murray, A. W. (1998) *J. Cell Biol.* **141,** 1193–1205.
29. Zou, H., McGarry, T. J., Bernal, T. & Kirschner, M. W. (1999) *Science* **285,** 418–422.
30. Rieder, C. L., Schultz, A., Cole, R. & Sluder G. (1994) *J. Cell Biol.* **127,** 1301–1310.
31. Jordan, M. A., Thrower, D. & Wilson L. (1992) *J. Cell Sci.* **102,** 401–416.
32. Li, X. & Nicklas, R. B. (1997) *J. Cell Sci.* **110,** 537–545.
33. Mitchison, T. J. (1989) *J. Cell Biol.* **109,** 637–652.
34. Dobles, M., Liberal, V., Scott, M. L., Benezra, R. & Sorger, P. K. (2000) *Cell* **101,** 635–645.